ACS APPLIED MATERIALS & INTERFACES

Research Article

www.acsami.org

Facile One-Step Photolithographic Method for Engineering Hierarchically Nano/Microstructured Transparent Superamphiphobic Surfaces

Tingjie Li,[†] Maxim Paliy,[†,‡] Xiaolong Wang,[†] Brad Kobe,[‡] Woon-Ming Lau,[‡,§] and Jun Yang*[,†]

[†]Department of Mechanical and Materials Engineering, The University of Western Ontario, London, Ontario N6A 5B9, Canada

[‡]Surface Science Western, The University of Western Ontario, London, Ontario N6G 0J3, Canada

[§]Chengdu Green Energy and Green Manufacturing Technology R&D Center, Sichuan, China 610207

Supporting Information

ABSTRACT: It is of great value to develop a simple, controllable, and scalable method of making superamphiphobic surfaces. Here we present a facile one-step photolithographic method to engineer superamphiphobic surfaces consisting of photoresist micropillars decorated with nanoparticles of the same photoresist. The surface or coating is optically transparent and versatile, and can be fabricated on a broad range of substrates including stretchable elastomers. During the development of the micropillar array, photoresist nanoparticles are spontaneously grown on the micropillars by a well-controlled emulsification process of the un-cross-linked residual photoresist. This creates a hierarchical structure with a re-entrant and convex morphology which is the key for superoleophobicity. The chemical bonding between the nanoparticles and the micropillars is strong producing a robust and durable coating. This facile method is scalable and industry-applicable for a variety of applications such as self-cleaning, antifouling, and deicing/antifrosting.

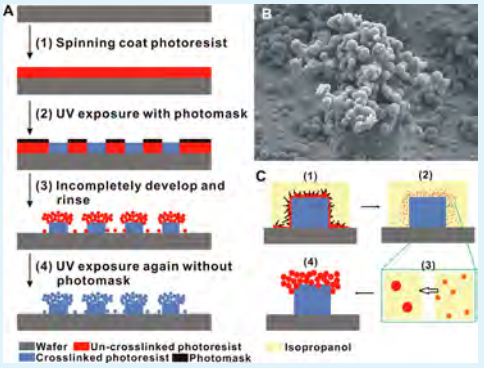

KEYWORDS: *superoleophobicity, superamphiphobicity, photolithography, hierarchical structure, photoresist, spontaneous emulsification*

INTRODUCTION

It is a challenge to create superamphiphobic surfaces which completely resist wetting not only by water, but also by organic liquids such as oils. While many surfaces found in nature, e.g., plant leaves, bird feathers, and insect legs/elytra/wings,[1−4] are superhydrophobic (super-repellent to water), no known natural surfaces are superoleophobic (super-repellent to oil). Recently a number of artificial superoleophobic surfaces have been engineered, with an oil (e.g., hexadecane) contact angle larger than 150°.[4−15] These surfaces have diverse potential applications such as self-cleaning, antifouling, deicing, antifrost, antifog, water/oil separation, drag reduction, and control of heat transfer.[12] However, typical preparation methods of such surfaces are complex and costly, and cannot be applied on a large scale. The difficulties are mostly related to the manufacturing of a robust hierarchical structure with re-entrant and convex morphology which is the key for superoleophobicity. Here we show a simple but robust, one-step photolithographic method for engineering transparent superoleophobic surfaces that can be deposited on a wide variety of substrates. Such surfaces consist of photoresist micropillars decorated with photoresist nanoparticles; the latter are grown *in situ* in the course of development of the micropillar array via a spontaneous emulsification process of the un-cross-linked residual photoresist.

The general concept to produce surfaces with ultralow wettability is well-known and relies on rough or textured surfaces instead of flat surfaces.[16,17] On a flat surface, the Young contact angle θ_{flat} is determined by Young's equation

$$\cos\theta_{flat} = (\gamma_{SV} - \gamma_{SL})/\gamma_{LV} \quad (1)$$

where γ denotes the surface energy/tension, and the subscripts S, L, and V stand for solid, liquid, and vapor, respectively [the solid−liquid surface tension can be estimated from the other two as follows, $\gamma_{SL} = \gamma_{SV} + \gamma_{LV} - 2(\gamma_{SV}\gamma_{LV})^{1/2}$[18]]. If we consider a flat solid surface terminated with $-CF_3$ groups, the one that has the lowest surface energy $\gamma_{SV} \sim 6$ mJ/m^2,[19] the Young's contact angles for oils are always less than 90°. For example, hexadecane has a surface energy of $\gamma_{LV} = 27.6$ mJ/m,^{2} and $\theta_{flat} \approx 80°$ (while for water $\theta_{flat} \approx 120°$).[20] In other words, all flat surfaces are intrinsically oleophilic, regardless of surface chemical composition. By contrast, on a rough or textured surface, a liquid droplet can be "impaled" on top of the roughness asperities, in a state of heterogeneous wetting. This mechanism can be described by the Cassie−Baxter[21] equation

Received: March 17, 2015
Accepted: May 5, 2015
Published: May 5, 2015

DOI: 10.1021/acsami.5b01926
ACS Appl. Mater. Interfaces 2015, 7, 10988−10992

$$\cos\theta^* = -1 + f(1 + \cos\theta_{flat}) \quad (2)$$

where θ^* is the apparent contact angle on the rough/textured surface and f is the fraction of solid surface area in contact with the liquid. If $f \ll 1$, a contact angle θ^* much larger than θ_{flat} (ultimately, $\theta^* \rightarrow 180°$ when $f \rightarrow 0$) and a low roll-off angle for the liquid droplet are achieved. Typically, if θ^* is larger than 150°, the surface is considered to be super-repellent. The first ingredient for superamphiphobicity is therefore a hierarchical surface morphology with multiscale (e.g., both micro- and nanoscale) roughness, ideally a fractal,[22,23] which can strongly reduce the value of f.

In contrast to superhydrophobicity, achieving superoleophobicity requires, however, a second crucial ingredient, a very specific surface morphology—re-entrant/overhanging surface features,[22,23] as explained below. Besides, a convex surface profile[16,24] is needed to stabilize the liquid−solid−vapor contact line. Hence, our approach to the design of the superamphiphobic coating is illustrated in Figure 1. The most

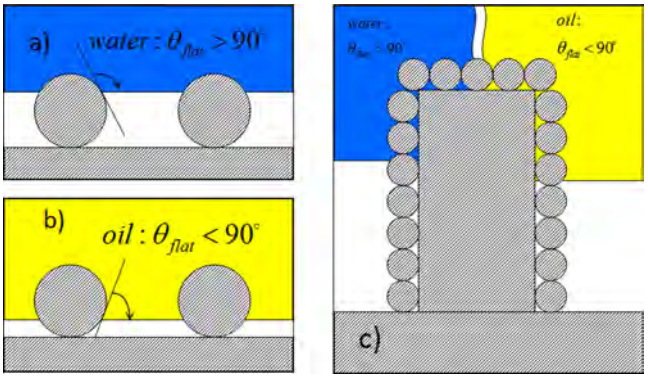

Figure 1. Basics of superamphiphobicity. (a) Water is pinned at the top halves of the spheres. (b) Oil can only be pinned at the lower parts of the spheres (overhanging/re-entrant features). (c) A very simple design of superamphiphobic surface combining re-entrancy and convexity, that we implement in our experiments.

generic shape that combines both convexity and re-entrancy is a sphere placed on a flat surface (Figure 1a,b). Comparison between parts a and b of Figure 1 clarifies why the re-entrant/overhanging feature of roughness is necessary for intrinsically oleophilic materials ($\theta_{flat} < 90°$) to make a superoleophobic surface. In our design, microscale pillars on the surface are decorated with nanospheres. Exclusion of a large fraction of the solid surface from contacting the liquid is first induced on a microscale with the micropillars and then further enhanced on a nanoscale with the nanospheres (Figure 1c). In this work, nanospheres are produced with a novel spontaneous emulsification process incorporated in the photoresist-based fabrication of the micropillars, as described in detail below.

RESULTS AND DISCUSSION

Making hierarchical and re-entrant structures is challenging. In pioneering studies, superoleophobic surfaces were produced via a range of methods, including chemical etching,[25,26] ion-etching,[27] anodizing,[28−30] electrodeposition,[31,32] template replication,[10,33] pyrolysis,[34−36] spray coating,[37,38] and photolithography.[11,15,39] Most of these methods are relatively complex and costly and cannot be applied to large scale substrates. Moreover, due to the practical problems including complicated fabrication processes that typically include many steps, limitation to certain substrates or chemicals, and poor mechanical flexibility and durability, commercial exploitation of superoleophobic surfaces has not been realized. Here we show a robust method that stems from simple conventional photolithography. Photolithography can produce regular photoresist patterns such as micropillar array. However, the micropillars lack re-entrant/overhanging features. We achieve superamphiphobicity by randomly decorating the tops of micropillars with spherical nanoparticles. The nanoparticles are subsequently cross-linked to micropillars to form robust multiscale re-entrant and convex structures. Such a surface becomes superamphiphobic after vapor fluorination. Compared to previous studies that involved multiple steps of micro/nanofabrication, our method includes only one simple step of photolithography, which greatly simplifies the fabrication process of a complex hierarchical and re-entrant morphology.

Figure 2A shows a schematic of the entire process for the fabrication of the nanoparticles-on-micropillars surface. The

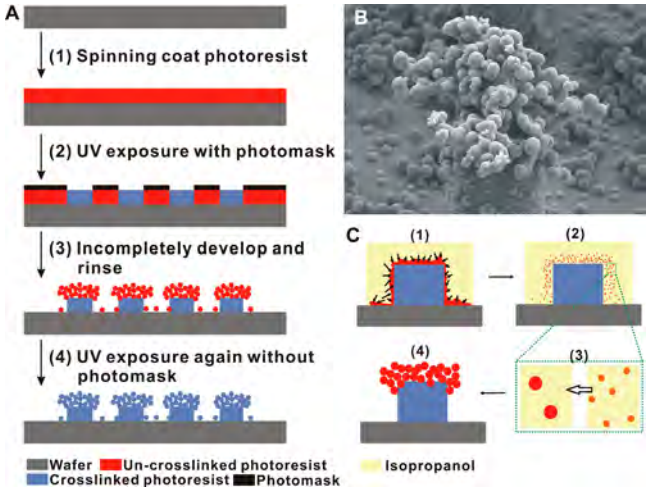

Figure 2. Schematic illustration of one-step photolithography process for engineering superamphiphobicity. (A) Process for the fabrication of micropillars decorated with nanoparticles to achieve superamphiphobicity. (B) SEM image of the nanoparticles' inlaid micropillar (6 μm in diameter). (C) Schematic showing the formation of nanoparticles by the "Ouzo effect", where (1) isopropanol diffuses into the residual un-cross-linked SU-8 solution in developer; (2) supersaturation of the SU-8 causes homogeneous nanometric size droplets; (3) diffusion of SU-8 into nearby droplets forms bigger droplets; (4) SU-8 droplets attach to pillars after isopropanol is removed.

negative photoresist (SU-8 3010) was spin-coated on a precleaned substrate, which was then baked at 95 °C to remove the excess solvent from the SU-8 layer. Next, the SU-8 layer was exposed to ultraviolet (UV) light through a photomask (sensor wavelength = 365 nm, UV intensity 6 mW/cm^2) for a specific duration. After polymerization of the SU-8 under postexposure baking, the sample was developed in SU-8 developer solution for a period shorter than the time normally required for fully washing away the un-cross-linked photoresist as described below. Finally, after the sample has been rinsed using isopropanol and dried, it was exposed to a UV lamp to fully cure the photoresist having the desirable hierarchical structure (Figure 2B). The key parameter here is the development time of the photoresist. By tuning the development time shorter than normally recommended for full

DOI: 10.1021/acsami.5b01926
ACS Appl. Mater. Interfaces 2015, 7, 10988−10992

development, some un-cross-linked residual photoresist is allowed to remain on the surface of polymerized micropillars after development. When the surface is rinsed with isopropanol, a liquid–liquid nucleation process occurs forming the photoresist nanoparticles. This process is similar to the Ouzo effect or spontaneous emulsification,[40−42] where a milky microemulsion forms when water is added to the liqueur Ouzo forming a ternary system of water, hydrophobic anise oils, and ethanol. In our case, the un-cross-linked photoresist solution forms spherical nanoparticles with the addition of isopropanol as an immiscible agent (Figure 2C). Here, the negative photoresist, developer, and isopropanol play roles similar to those of the anisole oil, ethanol, and water in Ouzo, respectively. When brought into contact with isopropanol, the negative photoresist solution in the developer becomes supersaturated, due to the diffusion of isopropanol into the solution and diffusion of developer out of the solution into the bulk isopropanol (so-called "solvent displacement" mechanism). This leads to the nucleation of photoresist nanodroplets. Subsequently, the supersaturation decreases until no further nucleation can occur.[40−42] Interestingly, in our experiments the nanoparticles were observed to mostly aggregate around the tops of the pillars instead of filling the gaps between the pillars (Figure 3A–D).

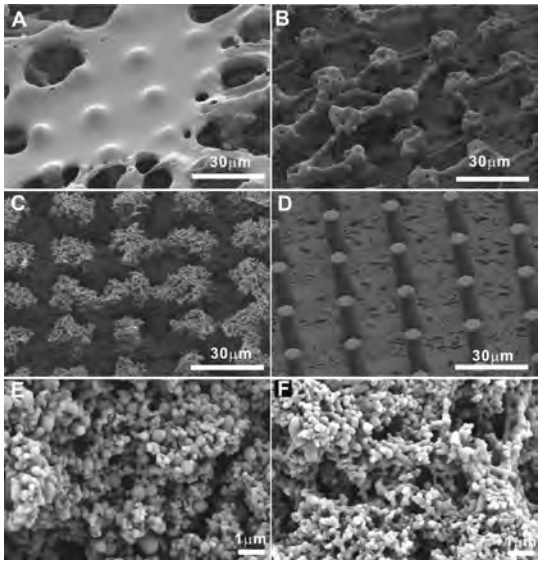

Figure 3. Hierarchical nanoparticle-on-micropillar structure of SU-8 pattern on Si wafer. (A–D) SEM images of the nanoparticles inlaid micropillar surfaces obtained at 30, 40, 60, and 90 s of development time, respectively. (E, F) High magnification SEM images showing the size dependence of the nanoparticles vs development time, 30 and 60 s, respectively.

We analyzed how the surface morphology changes with the development time, and concluded that, for the most efficient formation of the nanoparticles, there exists an optimum development time of about 60 s (Figure 3C). As observed by SEM, short development times (30–40 s, Figure 3A,B) result in a patchy film of un-cross-linked photoresist covering the top of the pillars. However, long development times exceeding 90 s show that most of the un-cross-linked photoresist has been washed away and almost no nanoparticles are formed (Figure 3D), leaving a smooth micropillar array (Supporting Information Figure S1). The size of the nanoparticles also depends on the development time. As shown in Figure 3E,F, the particles formed within 60 s of development time range in size from 200 to 400 nm in diameter, and they are smaller and more uniform than those with development times less 30 s (130–800 nm). After fluorination, all the surfaces depicted in Figure 3B–D are superhydrophobic. The static contact angles of water for these surfaces are all near 180° so that a water droplet rolls off under the smallest mechanical disturbance, and it is difficult to keep it steady on the surface. However, oils were found to behave differently on these surfaces. For a bare pillar surface (Supporting Information Figure S1), the static contact angle of hexadecane is ∼135°, and the droplet does not roll off when the surface is tilted and even turned over; i.e., the oil fills the valleys between the pillars. By contrast, the static contact angle of hexadecane on the nanoparticles/micropillars surface (Figure 3C) is ∼160°, and the hexadecane droplet rolls off easily with a sliding angle ≤10°. Methanol was observed to have a static contact angle of ∼120° (the measurement error for the contact angle was ∼2° in all cases). The qualitative change from superhydrophobicity to superoleophobicity and thus superamphiphobicity is attributed to the hierarchical and re-entrant structure comprising convex nanoparticles and micropillars, as was designed above (Figure 1). We emphasize that superamphiphobicity of the surface is versatile. It should manifest for a wide range of oils, provided their surface tension is not extremely low.

We have also studied how the superamphiphobic properties of the engineered surfaces depend on the area fraction of the pillars tops, f (relative to the total surface area). We prepared a set of surfaces with pillars of different diameter, from $d = 6$ μm (as in Figure 3) to $d = 14$ μm at constant pitch of $p = 25$ μm, which corresponded to a range of area fraction $f = \pi d^2/4p^2$ from $f = 0.045$ up to $f = 0.246$. Note that this estimation of the area fraction f is simplified as it does not account for the presence of the nanoparticles. As shown in Figure 4A, both for the bare micropillars and for the nanoparticles–micropillars surfaces, the contact angle for hexadecane monotonically decreases with f. One should note that the bare pillars' surface was never observed to be superoleophobic (i.e., the contact angle for oil is always <150°) no matter what the value of f was. By contrast, the nanoparticle–micropillar surface was observed to be superamphiphobic when $f < 0.12$. For all the studied values of f, the hierarchically textured surface showed high oil contact angles, and the oil droplets rolled off without leaving any trace of the oil on the surface, upon a slight inclination of the substrate on the order of 10° or less. For the nanoparticle–micropillar surface, the dependence of the hexadecane contact angle on f corresponds to the Cassie–Baxter equation for heterogeneous wetting (eq 2).[21] Indeed, the data for the pillars with the nanoparticles from Figure 4A (red line and circles) can be very precisely approximated via eq 2, as attested by Figure 4B. From the slope of the linear fit one can immediately find that $1 + \cos\theta_{flat} \approx 1.17 \pm 0.04$, i.e., $\theta_{flat} \approx 80 \pm 2°$. This value precisely matches the known value in the literature of the "flat" contact angle $\theta_{flat} \approx 80°$ for hexadecane on the CF_3-terminated surface.[43]

Tape tests were conducted to investigate the mechanical durability of the obtained superamphiphobic coatings. Because nanoparticles and micropillars consist of the same cross-linked negative photoresist, as verified by FTIR (Supporting Information Figure S2), the bonding between the nanoparticles and the micropillars is very strong, resulting in a very robust multiscale structure. We found that the surface could endure

DOI: 10.1021/acsami.5b01926
ACS Appl. Mater. Interfaces 2015, 7, 10988–10992

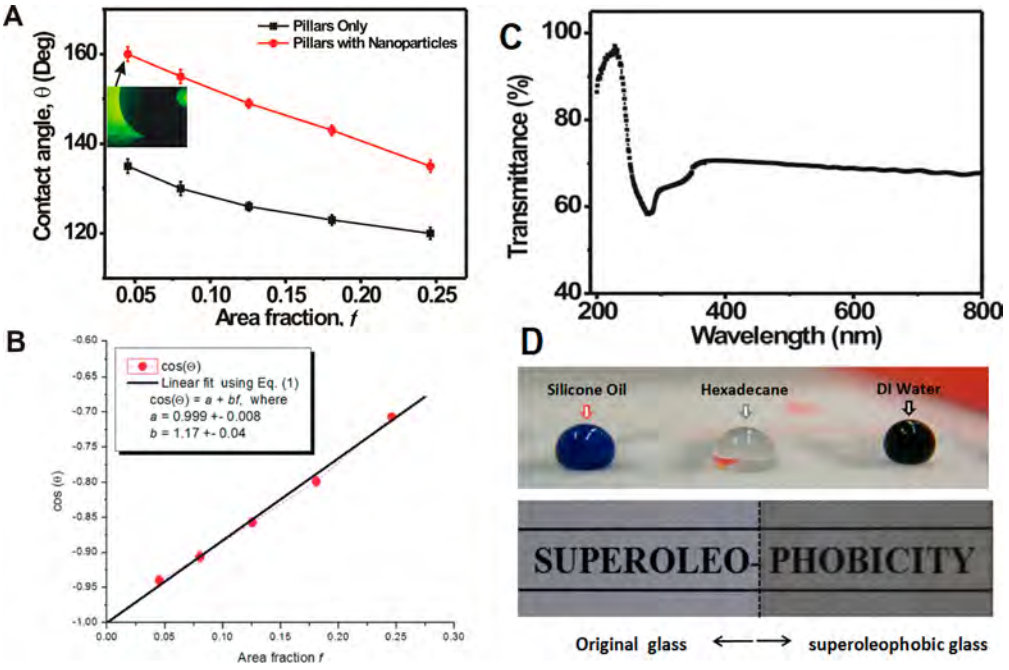

Figure 4. Hexadecane oil wettability and optical transparency of the SU-8 superamphiphobic coatings. (A) Contact angle as a function of area fraction for pillar only and nanoparticle/micropillar surface. (B) Fit of the data depicted in part A (nanoparticles/micropillars surface) via the Cassie–Baxter formula eq 2. (C) UV–vis spectrum showing the transparency of the superamphiphobic coating on the glass slide (pillars of ~50 μm in height, and ~6 μm in diameter). (D) Optical image of various liquids (silicon oil, blue; hexadecane, colorless; water, black) on the superoleophobic coated glass slide; transparency of the superoleophobic glass slide versus the original glass slide.

seven repetitions of tape tests, before the superoleophobicity was compromised to the extent that a hexadecane droplet could not roll off the surface (Supporting Information Table S1). Even then, the surface was still superhydrophobic with water contact angle >150° and the sliding angle <10°.

Nontransparency of coatings often limits their applications. Since the negative photoresist used is a transparent material, the resulting superamphiphobic surfaces are highly transparent as well. As verified by UV–vis spectrophotometer (Figure 4C), a pillar array with ~50 μm height retained 70% of transparency in the visible wavelength from 400 to 800 nm. One can easily read the letters underneath the superoleophobic surface coated glass (Figure 4D). The nearly perfect spherical shape of various liquid droplets further illustrates the excellent super-repellent properties of the coating. Note that the transparency of the surface should generally decrease with increasing the area fraction of pillars. The nanoparticles appear nontransparent, which is the major contributor to opacity. However, within the limited useful range of the area fraction of the pillars for superoleophobicity, $f < 0.12$, the transparency should not be affected drastically.

More importantly, the present photolithography-based method can be applied to other negative photoresists, such as KMPR. In addition, since negative photoresists possess high surface adhesion to various substrates, the present method for engineering superamphiphobic surfaces can be realized on a wide variety of substrate materials. To demonstrate its versatility, superamphiphobicity was achieved by this method using the KMPR photoresist, and on a range of substrates including elastomers and metals (Supporting Information Table S1). On elastomers, excellent superamphiphobicity can be maintained even during the stretching–releasing cycles up to 30% tensile strain (Supporting Information Figure S4).

CONCLUSION

In summary, we have developed a simple but versatile method to fabricate superamphiphobic surfaces, a method derived from conventional photolithography of forming an array of photoresist micropillars which can be made using common photoresists on a broad range of substrates. In the course of solution-based development of the photoresist micropillars, we engineered spontaneous emulsification of the photoresist (the "Ouzo effect") and made photoresist nanoparticles superimposed on top of the photoresist micropillars composed of the same material. This hierarchical design leads to the formation of a re-entrant and convex surface morphology that is essential for superoleophobicity. The bonding between the nanoparticles and pillars is very strong because of the chemical cross-links, endowing the superoleophobic surface high mechanical durability. Hexadecane can have contact angle larger than 160° on such surface, and the oil droplets can easily roll off when the surface is tilted by 10°. The superoleophobic layer is transparent and can be applied to a wide variety of substrates including metals, polymers, and elastomers. This simple but novel method for engineering superamphiphobic surfaces promises wide industrial applications in self-cleaning, antifouling, deicing/antifrosting etc.

ASSOCIATED CONTENT

Supporting Information

Details regarding materials and methods as well as supplementary Figures S1–S4, and Table S1. The Supporting Information is available free of charge on the ACS Publications website at DOI: 10.1021/acsami.5b01926.

DOI: 10.1021/acsami.5b01926
ACS Appl. Mater. Interfaces 2015, 7, 10988–10992

AUTHOR INFORMATION

Corresponding Author

*E-mail: jyang@eng.uwo.ca.

Notes

The authors declare no competing financial interest.

ACKNOWLEDGMENTS

This work was supported by The Ontario Research Fund Research Excellence (ORF-RE) program of Ministry of Research and Innovation, LANXESS Inc, the Natural Science and Engineering Research Council of Canada (NSERC) and the Canada Foundation for Innovation (CFI).

REFERENCES

(1) Barthlott, W.; Neinhuis, C. Purity of the Sacred lotus, or Escape from Contamination in Biological Surfaces. *Planta* **1997**, *202* (1), 1−8.

(2) Gao, X. F.; Jiang, L. Water-repellent Legs of Water Striders. *Nature* **2004**, *432* (7013), 36−36.

(3) Parker, A. R.; Lawrence, C. R. Water Capture by a Desert Beetle. *Nature* **2001**, *414* (6859), 33−34.

(4) Sun, T. L.; Feng, L.; Gao, X. F.; Jiang, L. Bioinspired Surfaces with Special Wettability. *Acc. Chem. Res.* **2005**, *38* (8), 644−652.

(5) Erbil, H. Y.; Demirel, A. L.; Avci, Y.; Mert, O. Transformation of a Simple Plastic into a Superhydrophobic Surface. *Science* **2003**, *299* (5611), 1377−1380.

(6) Genzer, J.; Efimenko, K. Creating Long-lived Superhydrophobic Polymer Surfaces Through Mechanically Assembled Monolayers. *Science* **2000**, *290* (5499), 2130−2133.

(7) Lafuma, A.; Quere, D. Superhydrophobic States. *Nat. Mater.* **2003**, *2* (7), 457−460.

(8) Liu, M. J.; Zheng, Y. M.; Zhai, J.; Jiang, L. Bioinspired Super-antiwetting Interfaces with Special Liquid-Solid Adhesion. *Acc. Chem. Res.* **2010**, *43* (3), 368−377.

(9) Yao, X.; Song, Y. L.; Jiang, L. Applications of Bio-Inspired Special Wettable Surfaces. *Adv. Mater.* **2011**, *23* (6), 719−734.

(10) Deng, X.; Mammen, L.; Butt, H. J.; Vollmer, D. Candle Soot as a Template for a Transparent Robust Superamphiphobic Coating. *Science* **2012**, *335* (6064), 67−70.

(11) Tuteja, A.; Choi, W.; Ma, M. L.; Mabry, J. M.; Mazzella, S. A.; Rutledge, G. C.; McKinley, G. H.; Cohen, R. E. Designing Superoleophobic Surfaces. *Science* **2007**, *318* (5856), 1618−1622.

(12) Vakarelski, I. U.; Patankar, N. A.; Marston, J. O.; Chan, D. Y.; Thoroddsen, S. T. Stabilization of Leidenfrost Vapour Layer by Textured Superhydrophobic Surfaces. *Nature* **2012**, *489* (7415), 274−7.

(13) Wong, T. S.; Kang, S. H.; Tang, S. K. Y.; Smythe, E. J.; Hatton, B. D.; Grinthal, A.; Aizenberg, J. Bioinspired Self-repairing Slippery Surfaces with Pressure-stable Omniphobicity. *Nature* **2011**, *477* (7365), 443−447.

(14) Liu, X. J.; Liang, Y. M.; Zhou, F.; Liu, W. M. Extreme Wettability and Tunable Adhesion: Biomimicking Beyond Nature? *Soft Matter* **2012**, *8* (7), 2070−2086.

(15) Tuteja, A.; Choi, W.; McKinley, G. H.; Cohen, R. E.; Rubner, M. F. Design Parameters for Superhydrophobicity and Superoleophobicity. *MRS Bull.* **2008**, *33* (8), 752−758.

(16) Quere, D. Non-sticking Drops. *Rep. Prog. Phys.* **2005**, *68* (11), 2495−2532.

(17) Quere, D. Wetting and Roughness. *Annu. Rev. Mater. Res.* **2008**, *38* (1), 71−99.

(18) Israelachvili, J. *Intermolecular and Surface Forces*; Academic Press: London, 1991.

(19) Adamson, A. W.; Gast, A. P. *Physical Chemistry of Surfaces*; Wiley: New York, 1997; pp 368.

(20) Mittal, K. L. *Contact Angle, Wettability and Adhesion*; VSP Intl Science: Leiden, The Netherlands, 2008; Vol. 5.

(21) Cassie, A. B. D.; Baxter, S. Wettability of Porous Surfaces. *Trans. Faraday Soc.* **1944**, *40*, 546−551.

(22) Herminghaus, S. Roughness-induced Non-wetting. *Europhys. Lett.* **2000**, *52*, 165.

(23) Shibuichi, S.; Yamamoto, T.; Onda, T.; Tsujii, K. Super Water-and-oil-repellent Surfaces Resulting from Fractal Structure. *J. Colloid Interface Sci.* **1998**, *208* (1), 287−294.

(24) Marmur, A. From Hygrophilic to Superhygrophobic: Theoretical Conditions for Making High-Contact-Angle Surfaces from Low-Contact-Angle Materials. *Langmuir* **2008**, *24* (14), 7573−7579.

(25) Meng, H. F.; Wang, S. T.; Xi, J. M.; Tang, Z. Y.; Jiang, L. Facile Means of Preparing Superamphiphobic Surfaces on Common Engineering Metals. *J. Phys. Chem. C* **2008**, *112* (30), 11454−11458.

(26) Cao, L. L.; Price, T. P.; Weiss, M.; Gao, D. Super Water- and Oil-repellent Surfaces on Intrinsically Hydrophilic and Oleophilic Porous Silicon Films. *Langmuir* **2008**, *24* (5), 1640−1643.

(27) Kumar, R. T. R.; Mogensen, K. B.; Boggild, P. Simple Approach to Superamphiphobic Overhanging Silicon Nanostructures. *J. Phys. Chem. C* **2010**, *114* (7), 2936−2940.

(28) Wang, X. L.; Liu, X. J.; Zhou, F.; Liu, W. M. Self-healing Superamphiphobicity. *Chem. Commun.* **2011**, *47* (8), 2324−2326.

(29) Wu, W. C.; Wang, X. L.; Wang, D. A.; Chen, M.; Zhou, F.; Liu, W. M.; Xue, Q. J. Alumina Nanowire Forests via Unconventional Anodization and Super-repellency Plus Low Adhesion to Diverse Liquids. *Chem. Commun.* **2009**, *9*, 1043−1045.

(30) Wang, D. A.; Wang, X. L.; Liu, X. J. E.; Zhou, F. Engineering a Titanium Surface with Controllable Oleophobicity and Switchable Oil Adhesion. *J. Phys. Chem. C* **2010**, *114* (21), 9938−9944.

(31) Xi, J. M.; Feng, L.; Jiang, L. A General Approach for Fabrication of Superhydrophobic and Superamphiphobic Surfaces. *Appl. Phys. Lett.* **2008**, *92* (5), 053102 −053102−3.

(32) Darmanin, T.; Guittard, F. Molecular Design of Conductive Polymers To Modulate Superoleophobic Properties. *J. Am. Chem. Soc.* **2009**, *131* (22), 7928−7933.

(33) Liu, X. J.; Wu, W. C.; Wang, X. L.; Luo, Z. Z.; Liang, Y. M.; Zhou, F. A Replication Strategy for Complex Micro/nanostructures with Superhydrophobicity and Superoleophobicity and High Contrast Adhesion. *Soft Matter* **2009**, *5* (16), 3097−3105.

(34) Zhang, J. P.; Seeger, S. Polyester Materials with Superwetting Silicone Nanofilaments for Oil/Water Separation and Selective Oil Absorption. *Adv. Funct. Mater.* **2011**, *21* (24), 4699−4704.

(35) Zhang, J. P.; Seeger, S. Superoleophobic Coatings with Ultralow Sliding Angles Based on Silicone Nanofilaments. *Angew. Chem., Int. Ed.* **2011**, *50* (29), 6652−6656.

(36) Zimmermann, J.; Rabe, M.; Artus, G. R. J.; Seeger, S. Patterned Superfunctional Surfaces Based on a Silicone Nanofilament Coating. *Soft Matter* **2008**, *4* (3), 450−452.

(37) Steele, A.; Bayer, I.; Loth, E. Inherently Superoleophobic Nanocomposite Coatings by Spray Atomization. *Nano Lett.* **2009**, *9* (1), 501−505.

(38) Wang, X. L.; Hu, H. Y.; Ye, Q.; Gao, T. T.; Zhou, F.; Xue, Q. J. Superamphiphobic Coatings with Coralline-like Structure Enabled by One-step Spray of Polyurethane/Carbon Nanotube Composites. *J. Mater. Chem.* **2012**, *22* (19), 9624−9631.

(39) Golovin, K.; Lee, D. H.; Mabry, J. M.; Tuteja, A. Transparent, Flexible, Superomniphobic Surfaces with Ultra-Low Contact Angle Hysteresis. *Angew. Chem., Int. Ed.* **2013**, *52* (49), 13007−13011.

(40) Anton, N.; Benoit, J. P.; Saulnier, P. Design and Production of Nanoparticles Formulated from Nano-emulsion Templates—A review. *J. Controlled Release* **2008**, *128* (3), 185−199.

(41) Ganachaud, F.; Katz, J. L. Nanoparticles and Nanocapsules Created Using the Ouzo Effect: Spontaneous Emulsification as an Alternative to Ultrasonic and High − Shear Devices. *ChemPhysChem* **2005**, *6* (2), 209−216.

(42) Vitale, S. A.; Katz, J. L. Liquid Droplet Dispersions Formed by Homogeneous Liquid-liquid Nucleation:"The Ouzo Effect. *Langmuir* **2003**, *19* (10), 4105−4110.

(43) Mittal, K. L. *Contact Angle, Wettability and Adhesion*; VSP Intl Science: Leiden, The Netherlands, 2008; Vol. 5.

DOI: 10.1021/acsami.5b01926
ACS Appl. Mater. Interfaces 2015, 7, 10988−10992